



# Adjustments to Proactive Motor Inhibition without Effector-Specific Foreknowledge Are Reflected in a Bilateral Upregulation of Sensorimotor $\beta$ -Burst Rates

Cheol Soh<sup>1</sup>, Megan Hynd<sup>1</sup>, Benjamin O. Rangel<sup>2</sup>, and Jan R. Wessel<sup>1,2</sup>

## Abstract

■ Classic work using the stop-signal task has shown that humans can use inhibitory control to cancel already initiated movements. Subsequent work revealed that inhibitory control can be proactively recruited in anticipation of a potential stop-signal, thereby increasing the likelihood of successful movement cancellation. However, the exact neurophysiological effects of proactive inhibitory control on the motor system are still unclear. On the basis of classic views of sensorimotor  $\beta$ -band activity, as well as recent findings demonstrating the burst-like nature of this signal, we recently proposed that proactive inhibitory control is implemented by influencing the rate of sensorimotor  $\beta$ -bursts during movement initiation. Here, we directly tested this hypothesis using scalp EEG recordings of  $\beta$ -band activity in 41 healthy human adults during a bimanual RT task. By comparing motor responses

made in two different contexts—during blocks with or without stop-signals—we found that premovement  $\beta$ -burst rates over both contralateral and ipsilateral sensorimotor areas were increased in stop-signal blocks compared to pure-go blocks. Moreover, the degree of this burst rate difference indexed the behavioral implementation of proactive inhibition (i.e., the degree of anticipatory response slowing in the stop-signal blocks). Finally, exploratory analyses showed that these condition differences were explained by a significant increase in  $\beta$  bursting that was already present during baseline period before the movement initiation signal. Together, this suggests that the strategic deployment of proactive inhibitory motor control is implemented by upregulating the tonic inhibition of the motor system, signified by increased sensorimotor  $\beta$ -bursting both before and after signals to initiate a movement. ■

## INTRODUCTION

Inhibitory control is a fundamental cognitive control ability that supports the implementation of many flexible and adaptive behaviors. In the motoric domain, inhibitory control allows humans to stop a movement outright, even if that movement has already been initiated. In the real world, this ability can help humans adapt their behavior to a rapidly changing environment—be it by stopping to walk into the street when suddenly noticing a previously overlooked car or by stopping to pick up a berry when realizing that a snake is lurking in the underwood. In the laboratory, the ability to implement inhibitory control is most often studied in the stop-signal task (SST; Verbruggen et al., 2019; Logan, Cowan, & Davis, 1984). In this task, participants first initiate an action to a go-signal that is presented on every trial. On some trials, a second signal—the stop-signal—is then presented with some delay after the initial go-signal, and participants have to attempt to cancel their response to the go-signal.

Subsequent work using this experimental paradigm has shown that successful action stopping in the SST depends on a mixture of two types of inhibitory control processes:

reactive and proactive (Braver, 2012). Reactive inhibition is triggered by the stop-signal itself, whereas proactive processes are recruited before the stop-signal, in anticipation of potentially having to cancel the movement (Wessel, 2018; Elchlepp, Lavric, Chambers, & Verbruggen, 2016; Aron, 2011; Verbruggen & Logan, 2009). In real-world scenarios, proactive inhibitory control is evident by the increase in motor caution that is exerted in some environmental contexts. For example, when approaching a busy intersection, humans may slow their walk in anticipation of an approaching vehicle. Similarly, when foraging in dense foliage, they may more cautiously grasp for foods in anticipation of potentially lurking carnivorous reptiles. To emulate such proactive control behaviors in the laboratory, researchers typically compare responses made in experimental blocks in which participants are instructed to expect no stop-signals (i.e., a pure-go RT task) to blocks in which stop-signals are expected (i.e., the classic SST design). Using this approach, studies have consistently found that go-responses made in stop-signal blocks are made more slowly compared to go-responses made in pure-go blocks, reflecting the heightened motor caution that humans exert when they anticipate potentially having to stop in the real world (Swann et al., 2012; Chikazoe et al., 2009; Jahfari, Stinear, Claffey, Verbruggen, & Aron, 2009;

<sup>1</sup>University of Iowa, <sup>2</sup>University of Iowa Hospital and Clinics

Verbruggen & Logan, 2009). Crucially, such studies also consistently found that the engagement of proactive inhibitory control directly benefits the implementation of reactive inhibitory control: Specifically, participants who show greater degrees of anticipatory motor slowing in stop-signal blocks also show faster stop-signal RTs (SSRTs). This also suggests that humans can strategically balance the degree to which they rely on either proactive or reactive control mechanisms (Braver, 2012), depending, for example, on how strongly they prioritize successful stopping compared to fast responding (Greenhouse & Wessel, 2013) or on how high they deem the relative likelihood of a stop-signal to be on a given trial (Vink, Kaldewaij, Zandbelt, Pas, & du Plessis, 2015).

With regard to the neural basis of inhibitory control, cognitive neuroscience has contributed much to our knowledge of how both reactive and proactive inhibitory control are implemented in the brain. The study of the basic stop-signal paradigm has elucidated a fronto-BG network of brain regions that is activated by stop-signals and implements reactive inhibitory control (for reviews, see Schmidt & Berke, 2017; Wessel & Aron, 2017; Jahanshahi, Obeso, Rothwell, & Obeso, 2015; Aron, Robbins, & Poldrack, 2014; Ridderinkhof, Forstmann, Wylie, Burle, & van den Wildenberg, 2011; Robbins, 2007). The neural underpinnings of proactive inhibitory control, however, are comparatively less clearly defined (Meyer & Bucci, 2016; Kenemans, 2015; Aron, 2011). Broadly speaking, studies either report that proactive inhibitory control is implemented via the anticipatory recruitment of the same control circuitry that is underlying reactive inhibitory control (e.g., Cunillera, Brignani, Cucurell, Fuentemilla, & Miniussi, 2016; Cai et al., 2015; Cunillera, Fuentemilla, Brignani, Cucurell, & Miniussi, 2014; Swann et al., 2012; Jahfari et al., 2009), via the attentional tuning of sensory processes that help detect potential stop-signals (e.g., Elchlepp et al., 2016; Kenemans, 2015), or via entirely separate neural circuitry (e.g., Cai, Chen, Ide, Li, & Menon, 2016; Vink et al., 2015; Majid, Cai, Corey-Bloom, & Aron, 2013; Zandbelt & Vink, 2010; Jaffard et al., 2008)—with many studies finding a mixture of these patterns. The most informative insights into the implementation of proactive inhibitory control come from studies that relate its purported neural signatures to its behavioral expression—that is, they show a systematic relationship between the relative slowing of motor responses in the stop-signal context (from here forward referred to as “proactive RT slowing”) and the purported neural signature of proactive inhibition. In one of the earliest studies of this type, Chikazoe et al. (2009) found that, across participants, the degree of neural activity within the reactive control network after stop-signals was inversely related to the degree of their proactive RT slowing. This provided one of the first pieces of neuroscientific support for the notion that the behavioral recruitment of proactive inhibition reduces the demand on the neural reactive inhibition system when movement cancellation is needed. Using a similar approach, Jahfari et al. (2009) have found

that proactive RT slowing was correlated with increased activity in a broad and distributed array of control-related frontoparietal brain regions activated on go-trials—most notably prefrontal brain regions that are also active during reactive control. This finding supports the view that proactive control can be implemented by an anticipatory recruitment of reactive control circuitry (but likely also involves additional structures and processes).

Further studies have lent additional evidence to the view that proactive inhibitory control is not purely attributable to the tuning of attentional processes that support stop-signal detection, but can instead directly affect the activity of the motor system. In that vein, studies using TMS have found that the recruitment of proactive inhibitory control can override the broad, nonselective suppression of motor excitability that is typically found during the reactive period after the stop-signal, thereby helping participants to more selectively target specific parts of the motor system when executing a stop (Duque, Greenhouse, Labruna, & Ivry, 2017; Greenhouse, Oldenkamp, & Aron, 2011). However, notably, the vast majority of studies that measure such changes in corticospinal excitability during the proactive control period use “foreknowledge” paradigms—that is, tasks in which participants know ahead of their motor initiation which specific motor effector they ultimately may have to stop (Cai, George, Verbruggen, Chambers, & Aron, 2012; Greenhouse et al., 2011; Majid, Cai, George, Verbruggen, & Aron, 2011; Claffey, Sheldon, Stinear, Verbruggen, & Aron, 2010). By utilizing this additional information, participants are able to selectively inhibit the critical effector without affecting the rest of the motor system (for reviews, see Duque et al., 2017; Aron, 2011). In contrast to this well-established literature on proactive, selective inhibition under conditions of foreknowledge, much less is known about whether (and how) proactive control affects the motor system when the to-be-inhibited motor effector is not known ahead of time—that is, when responses have to be made under a “global” state of caution and inhibition and cannot be targeted at a previously known, specific motor representation. Moreover, the neurophysiological changes that are underlying these observed changes in motor system excitability because of proactive control are still largely unknown.

In the latter respect, the neurophysiological activity of the sensorimotor cortex can be noninvasively investigated using scalp EEG. A substantial literature of existing research has consistently shown that the sensorimotor cortices display prominent activity in the  $\beta$ -frequency band ( $\sim 15$ – $29$  Hz). This  $\beta$ -band activity is suppressed leading up to and during movement (Tzagarakis, West, & Pellizzer, 2015; Kilavik, Zaepffel, Brovelli, MacKay, & Riehle, 2013; Pogosyan, Gaynor, Eusebio, & Brown, 2009; Schoffelen, Oostenveld, & Fries, 2008; Zhang, Chen, Bressler, & Ding, 2008; Baker, 2007; Neuper, Wörtz, & Pfurtscheller, 2006; Pfurtscheller, Graimann, Huggins, Levine, & Schuh, 2003; McFarland, Miner, Vaughan, & Wolpaw, 2000) and is directly related to corticospinal excitability (Schulz,

Übelacker, Keil, Müller, & Weisz, 2013). There are several proposed neurophysiological and functional interpretations of  $\beta$ -band activity during movement (e.g., Kilavik et al., 2013; Engel & Fries, 2010). One of the earliest and most enduring ideas is the proposal that sensorimotor  $\beta$ -band activity reflects a net-inhibited state of the motor system (Schulz et al., 2013; Pfurtscheller, Neuper, Flotzinger, & Pregenzer, 1997). Concomitantly, its reduction during movement initiation purportedly reflects the net disinhibition of the motor system in preparation for movement.

Building on that theory, two recent stop-signal studies have proposed that proactive inhibitory control may be implemented via a preparatory upregulation of sensorimotor  $\beta$ -band activity (Wessel, 2020; Muralidharan, Yu, Cohen, & Aron, 2019). Muralidharan et al. (2019) showed that, when foreknowledge is present, the selective, effector-specific proactive inhibitory control that is typically found in such paradigms is indexed by increased  $\beta$ -band activity over the contralateral sensorimotor site. Conversely, the Wessel (2020) study used a standard SST without foreknowledge, where inhibition cannot be targeted at a specific motor effector ahead of time. In that study, we first showed that trial-to-trial  $\beta$ -band activity in the sensorimotor cortex occurs in brief, transient bursts, rather than in the form of steady oscillations (which is in line with recent findings from the animal literature; cf. Sherman et al., 2016; Feingold, Gibson, DePasquale, & Graybiel, 2015). We then showed that the rate of these  $\beta$  bursts steadily declines in the lead-up to the movement, mirroring previous findings from the classic, power-based  $\beta$  literature (reviewed above). Crucially, we then found that the amount of sensorimotor  $\beta$ -bursts in the early premovement period positively predicted go-trial RT (more sensorimotor  $\beta$ -bursts = longer RTs) and negatively predicted SSRT (more bursts = faster SSRT). Therefore, we tentatively proposed that early sensorimotor  $\beta$ -bursting on go-trials could reflect the degree to which participants engaged general, nonspecific proactive inhibition of all potential responses.

However, although this study employed a large sample size of over 200 participants and therefore revealed reliable brain-behavior associations, the standard SST used therein did not include a pure-go condition to provide a control comparison without proactive inhibition. Hence, it was impossible to definitively conclude that early sensorimotor  $\beta$ -bursting truly reflects an active, strategic deployment of general proactive control. Indeed, a plausible alternative explanation is that some participants may innately show higher sensorimotor  $\beta$  bursting (i.e., a more strongly inhibited motor system overall), which would lead them to show longer RTs in general (i.e., a slower go-process), not just within the context of an SST. In the stop-signal context, then, participants with such a slowed go-process would have a systematic bias in the “race” between the stop-process and the go-process, resulting in more efficient reactive stopping (indexed by shorter SSRT). In that scenario, the observed direct relationship between  $\beta$ -bursts and both go- and stop-signal RTs could be explained

without any relationship between proactive inhibitory control and  $\beta$ -band activity.

Therefore, in the current study, we set out to directly test whether increases in sensorimotor  $\beta$ -bursts actually reflect a genuine strategic deployment of proactive inhibitory control. As in previous studies of proactive control in the absence of effector-specific foreknowledge (Wessel, Conner, Aron, & Tandon, 2013; Swann et al., 2012), participants ( $n = 41$ ) alternated between performing blocks of the SST and a pure-go task. We used scalp EEG to measure sensorimotor  $\beta$ -burst rates during go-trials performed in both contexts and aimed to directly test whether sensorimotor  $\beta$ -burst rates contralateral and/or ipsilateral to the response hand were increased in the stop-signal context compared to the pure-go context. We also aimed to relate these changes in sensorimotor  $\beta$ -bursting to proactive RT slowing. Finally, we aimed to explore whether the purported increase in  $\beta$ -bursting during the stop-signal blocks was specific to the period immediately after the go-signal (suggesting a strategic, transient deployment of proactive control specific to the movement initiation period) or whether such increases were found even before the go-signal was presented (suggesting a more broad control state that is sustained throughout the task).

## METHODS

### Data Availability

All data, analysis scripts, and task codes can be downloaded from the Open Science Framework at <https://osf.io/49hts/>.

### Participants

Forty-one healthy adult participants (27 women) participated in this study (mean age = 21.6 years,  $SD = 3.85$ , range = 18–30 years) in exchange for either class credit or an hourly compensation of \$15. All procedures were approved by the University of Iowa’s institutional review board (IRB #201511709). The same data were used to investigate a hypothesis about the fronto-central P3 event-related potential in the context of reactive inhibitory control (Hynd, Soh, Rangel, & Wessel, 2021).

### Stimulus Presentation

All stimuli were presented on a 19-in. Dell flat-screen monitor connected to an IBM-compatible PC running Fedora Linux and MATLAB 2015b (The MathWorks, Inc.). Stimuli were presented using Psychtoolbox 3 (Brainard, 1997). Responses were made using a standard QWERTY USB keyboard.

### Experimental Task

Stimuli were presented on a gray background (Figure 1). Each trial began with a black fixation cross (500 msec),

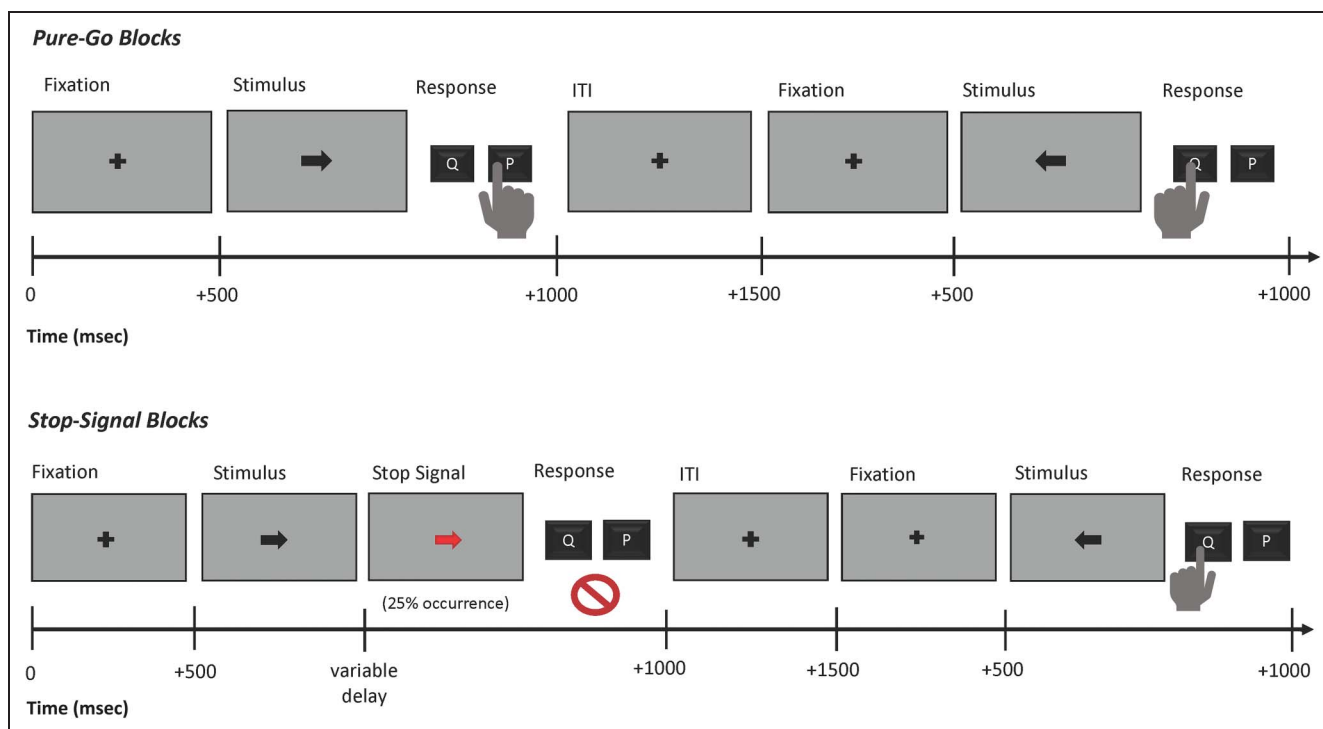


**Figure 1.** Task diagram.

followed by a black arrow (go-signal) pointing either left or right, displayed for 1000 msec. Participants were instructed to press the “q” key on the keyboard with their left index finger in case of a left-facing arrow and “p” with their right index finger in case of a right-facing arrow. Responses were to be made within the 1000-msec window during which the stimulus was presented on the screen. Each trial was followed by a 1500-msec intertrial interval. If no response was made during the response window, the first 1000 msec of the intertrial interval included a red “Too Slow!” message presented on the screen. In stop-signal blocks, a stop-signal (i.e., the black go-signal arrow changing to red color) was presented after the go-signal on 25% of trials. The stop-signal delay was initially set to 200 msec and was then subsequently adjusted in steps of 50 msec (which were added to the stop-signal delay after successful stop-trials and subtracted after failed stop-trials), with the goal of achieving an overall  $p(\text{stop})$  of approximately .5. Participants completed two blocks of practice with the SST and then performed 10 total blocks, alternating between stop-signal blocks (“There will be stop-signals. Responding quickly on go-trials and stopping successful on stop-trials are equally important.”) and pure-go blocks (“There will be no stop-signals. Respond as fast as possible.”). We altered the type of the first block after each participant to counterbalance the order. To achieve a balanced number of go-trials from each task context, each block contained 48 go-trials. In addition, the stop-signal blocks contained 16 stop-trials. In total, this resulted in 240 go-trials from pure-go blocks, 240 go-trials from stop-signal blocks, and 80 stop-trials per participant.

## Behavioral Analysis

Variables of interest were go-trial RT from both task contexts and SSRT, failed stop RT, and  $p(\text{stop})$  from the stop-signal blocks. Within the stop-blocks, go- and failed stop-trial RTs were compared to ensure that the requirements of the horse race model were met (failed stop RT < go-trial RT; Logan et al., 1984).  $p(\text{Stop})$  was investigated to ensure that the stop-signal delay staircase algorithm was effective in achieving an approximate stopping success rate of .5. SSRT was calculated using the integration method with replacement of go-trial omission errors (Verbruggen et al., 2019).

The primary behavioral variable of interest to the main hypothesis was the relative slowing of go-trial RT that was expected in stop-signal blocks compared to pure-go blocks (proactive RT slowing). First, these go-trial RTs from both task contexts were compared with a paired-samples  $t$  test. For the purposes of the brain-behavior correlation, a normalized proactive RT slowing value was then computed for each participant. We used a percent-change measure that normalizes the RT condition difference by the pure-go-trial RT, to account for baseline differences in RT. The resulting formula:

$$\text{Proactive RT slowing} = 100 * (\text{stop-signal block go-RT} - \text{pure-go block go-RT}) / \text{pure-go block go-RT}$$

expresses proactive RT slowing as the percentage of slowing found in stop-signal blocks relative to pure-go blocks.

### EEG Recording and Preprocessing

These steps were performed exactly as described in our recent paper (Wessel, 2020). The description is adapted from therein. In brief, we will discuss them below.

Scalp EEG was recorded using a 64-channel active EEG system (BrainProducts actiChamp). The ground was placed at electrode Fz, and the reference was placed at electrode Pz. Sampling rate was 500 Hz, with hardware filters set to time-constant high-pass 10 sec and low-pass 1000 Hz.

Data were preprocessed using custom routines in MATLAB, incorporating functions from EEGLAB (Delorme & Makeig, 2004). The data were imported into MATLAB and then filtered using symmetric two-way least-squares finite impulse response filters (high-pass cutoff: 0.3 Hz, low-pass cutoff: 30 Hz). Nonstereotyped artifacts were automatically removed from further analysis using segment statistics applied to each second-long segment of data joint probability and joint kurtosis, with both cutoffs set to 5 SDs (cf. Delorme, Sejnowski, & Makeig, 2007). Trials that included a rejected data segment were excluded from further analysis. After removal of nonstereotypic artifacts, the data were rereferenced to common average and subjected to a temporal infomax independent component analysis (Bell & Sejnowski, 1995), with extension to sub-Gaussian sources (Lee, Girolami, & Sejnowski, 1999). Components representing eye-movement and electrode artifacts were identified using outlier statistics and were removed from the data, alongside nondipolar components' residual variance cutoff at 15% (Delorme, Palmer, Onton, Oostenveld, & Makeig, 2012). The remaining components were back-projected into channel space and subjected to further analyses. The data were then transformed to a reference-free montage using the current source density (CSD) method (Tenke & Kayser, 2005; Perrin, Pernier, Bertrand, & Echallier, 1989).

### $\beta$ -Burst Detection

Sensorimotor  $\beta$ -bursts from go-trials in both contexts were quantified at electrode sites C3 and C4 from the CSD-converted montage.  $\beta$ -burst detection was performed as described in Shin, Law, Tsutsui, Moore, and Jones (2017) and implemented in our previous paper for human scalp EEG (Wessel, 2020). The description is adapted from therein.

First, each electrode's data were convolved with a complex Morlet wavelet of the form:

$$w(t, f) = A \exp\left(-\frac{t^2}{2\sigma_t^2}\right) \exp(2i\pi ft)$$

with  $\sigma = \frac{m}{2\pi f}$ ,  $A = \frac{1}{\sigma_t} \sqrt{2\pi}$ , and  $m = 7$  (cycles) for each of 15 evenly spaced frequencies spanning the  $\beta$ -band (15–29 Hz). Time–frequency power estimates were extracted by calculating the squared magnitude of the complex wavelet-convolved data. These power estimates were then epoched relative to the events in question (ranging from  $-500$  to  $+1000$  msec with respect to go-signals). Individual  $\beta$ -bursts were defined as local maxima in the trial-by-trial  $\beta$ -band time–frequency power matrix for which the power exceeded a set cutoff of  $6\times$  the median power of the entire time–frequency epoch power matrix for that electrode (i.e., the median thresholding was performed across all epochs). Local maxima within each 1500-msec epoch were identified using the MATLAB function *imregional()*. Example trials from one participant are depicted in Figure 2. Although the median thresholding procedure provides a rather coarse and simplistic threshold that is invariant across participants, this procedure matches work in both magnetoencephalography (Shin et al., 2017) and EEG (Wessel, 2020). Hence, this approach is consistent with existing literature—although further method development in this regard is necessary to identify more sophisticated and flexible  $\beta$ -burst detection procedures.

### Statistical Analyses

As in our previous study (Wessel, 2020), the rate of  $\beta$ -bursts at both electrode sites was quantified in bins, time-locked to the onset of the go-signal. This binning procedure was performed after the initial burst detection (described above)—that is, each burst was uniquely assigned to one bin according to its timing. Each of the five bins was 100 msec in length, together spanning the first 500 msec after the go-signal. This bin size was chosen because it represented an ideal trade-off between the dynamics of the sensorimotor  $\beta$ -burst counts and the amount of statistical tests to be performed. Within each bin, we compared the amount of sensorimotor  $\beta$ -bursts using a  $2 \times 2$  repeated-measures ANOVA with the two factors Context (stop-signal vs. pure-go blocks) and Side (contralateral vs. ipsilateral to the cued response). Because this resulted in five separate ANOVAs (one for each bin), the resulting  $p$  values were corrected for multiple comparisons using the false discovery rate procedure (FDR; Benjamini, Krieger, & Yekutieli, 2006).

Moreover, to test whether the purported increase in sensorimotor  $\beta$ -bursts was sustained throughout the entire stop-signal block or whether sensorimotor  $\beta$ -bursts were specifically upregulated during movement initiation, we also compared the amount of  $\beta$ -bursts in the baseline fixation period (500 msec before the go-signal) between both conditions. This was done using a paired-samples  $t$  test (because this measurement was taken before the go-signal, Laterality was not a factor in this analysis). To enable a comparison of this measurement to the burst rates during the 100-msec post-go-signal bins, this measurement was

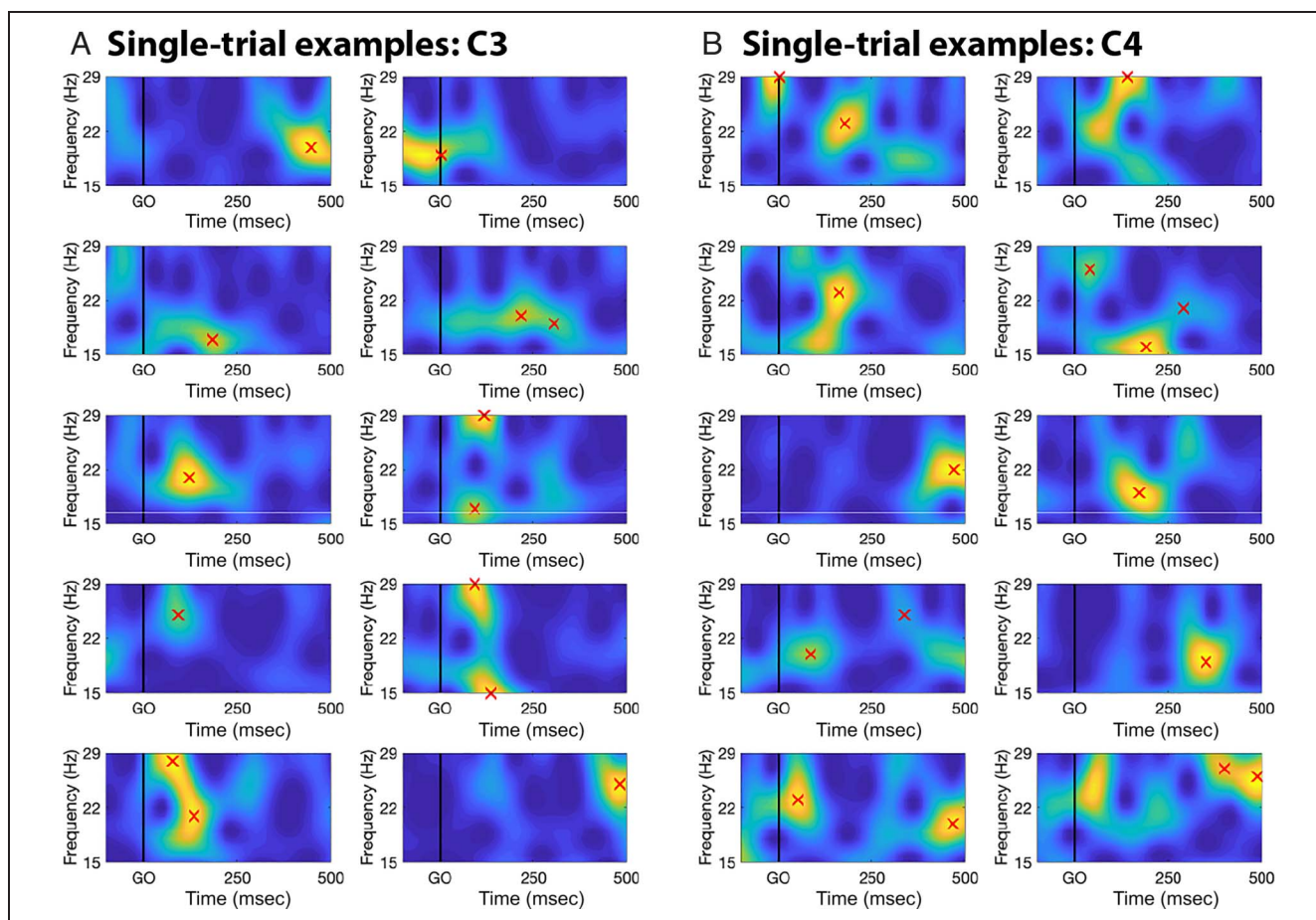


**Figure 2.** Demonstration of the burst detection procedure using a random selection of example trials from one random participant, focused on the  $\beta$ -band. Red crosses mark detected bursts.

converted into “ $\beta$ -bursts per 100 msec” by dividing the number of  $\beta$ -bursts in the 500-msec fixation period by a factor of 5.

We tested two types of brain–behavior relationships using Pearson’s product–moment correlation coefficient. First, to confirm that sensorimotor  $\beta$ -bursts are meaningfully related to movement initiation in both task contexts, we aimed to replicate our previous finding of a positive cross-participant correlation between the amount of early contralateral  $\beta$ -bursts on go-trials and go-trial RT (Wessel, 2020). We tested this correlation for each of the five bins and the two task contexts separately, correcting the resulting  $p$  values for multiple comparisons using the FDR method. We expected a positive correlation in the early bins in both task contexts.

Second, to test the main brain–behavior hypothesis regarding the relationship between the hypothesized general  $\beta$ -burst upregulation in the stop-signal blocks and the behavioral expression of proactive control, we identified the bins in which the main  $2 \times 2$  ANOVA revealed a main effect of Context and no influence of Laterality. The mean  $\beta$ -burst counts from these bins were then converted to the same percent-increase measure that was used for the behavioral

go-RT data. The following formula was used to quantify this measurement for each participant:

$$\beta\text{-burst increase} = 100 \times \frac{(\text{stop-signal block } \beta\text{-bursts} - \text{pure-go block } \beta\text{-bursts})}{\text{pure-go block } \beta\text{-bursts}}.$$

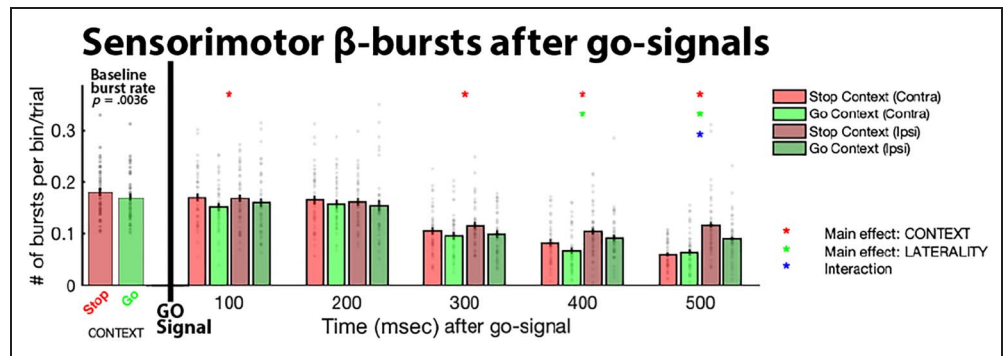
We hypothesized that there would be a significantly positive correlation between the percentage of increase in sensorimotor  $\beta$ -bursting found on stop-signal versus pure-go blocks and proactive RT slowing (quantified as explained in the Behavioral Analysis section).

## RESULTS

### Behavior

In line with the predictions from the horse race model of the SST, all participants showed longer go-trial RTs (mean = 553 msec,  $SD = 117$ ) compared to failed stop-trial RTs (mean = 488 msec,  $SD = 114$ ) in the stop-signal blocks.

**Figure 3.** Sensorimotor  $\beta$ -bursts in five consecutive time bins after go-signals in both task contexts, separately for contralateral (Contra) and ipsilateral (Ipsi) electrode sites, as well as during the pre-go baseline period (where the bars express  $\beta$ -burst rate per 100 msec to match the scaling of the post-go period). Gray dots represent individual participant means; black bars denote the standard error of the group mean. Asterisks denote significance of the respective main effect or interaction within the specified bin, corrected for multiple comparisons using FDR to a family-wise  $p < .05$ . For the baseline period, the exact  $p$  value (.0036) is listed above the bar plot.



$p(\text{stop})$  was .53 ( $SD = .05$ ), indicating the effectiveness of the staircase procedure. Mean SSRT was 237 msec ( $SD = 30$ ).

In line with our hypothesis and prior studies, go-trial RT was strongly affected by task context (stop-signal blocks: 553 msec,  $SD = 117$ ; pure-go blocks: 393 msec,  $SD = 50$ ;  $t(40) = 10.16$ ,  $p = 1.21 \times 10^{-12}$ ,  $d = 1.81$ ), indicating an average percent increase of 41.23% ( $SD = 27\%$ ) that ranged from 2.26% to 108% in individual participants.

### Post-go Sensorimotor $\beta$ -Burst Condition Averages

In line with our main hypothesis, sensorimotor  $\beta$ -bursts were increased in stop-signal blocks compared to pure-go blocks (Figure 3), moreover at both contralateral and ipsilateral electrode sites. After FDR correction, there was a significant main effect of Context in Bins 1 and 3–5. Moreover, in line with our previous report (Wessel, 2020), the contralateral electrode site showed lower  $\beta$ -burst rates in the bins toward the end of the prereponse period, resulting in a significant main effect of Laterality in Bins 4 and 5 and a significant Context  $\times$  Laterality interaction in Bin 5. Notably, no effect of Laterality was found during the early bins, showing that  $\beta$ -bursts were increased in the stop-signal context over both the ipsilateral and contralateral electrode sites. Test statistics and  $p$  values for all three factors across the five bins can be found in Table 1.

In response to a reviewer suggestion, we also explored other burst parameters (burst duration, frequency range, and power), although these variables have not been found to relate to behavior to the same extent as burst rate (Shin et al., 2017). Indeed, neither burst duration nor burst power showed any FDR-corrected significant task context effects in either of the windows. Burst frequency range did show a significant increase in the stop-signal context in the 200- to 300-msec window ( $p = .004$ ,  $\eta^2 = .19$ ). Although we had no a priori hypothesis regarding the interpretation of the burst frequency range parameter, one possible explanation for this result could be that the increase in burst rate in this window could lead to instances in which two bursts occur in neighboring frequency bands, with only one exceeding the median power threshold for detection (cf. top right trial example in Figure 2). However, at this point, this is conjectural.

### Brain–Behavior Correlations: $\beta$ -Burst Rates vs. Basic RT

Replicating our previous investigation (Wessel, 2020), early contralateral  $\beta$ -bursts after the go-signal predicted RT across participants (Figure 4). Importantly, extending those earlier findings, this was true for both task contexts, showing that there is a general relationship between

**Table 1.** Test Statistics for Bin-Wise ANOVAs of Sensorimotor  $\beta$ -Bursts After Go-Signals

Bin	Variable	Variable								
		Context			Laterality			Interaction		
		<i>F</i>	<i>p</i>	$\eta^2$	<i>F</i>	<i>p</i>	$\eta^2$	<i>F</i>	<i>p</i>	$\eta^2$
0–100	<b>4.29</b>	<b>.04</b>	<b>.10</b>	0.43	.51	.01	0.97	.33	.02	
100–200	1.54	.22	.04	0.39	.54	.01	0.01	.91	.00	
200–300	<b>6.37</b>	<b>.02</b>	<b>.14</b>	2.86	.10	.07	0.93	.34	.02	
300–400	<b>6.42</b>	<b>.02</b>	<b>.14</b>	<b>16.68</b>	<b>.00</b>	<b>.29</b>	0.07	.79	.00	
400–500	<b>4.95</b>	<b>.03</b>	<b>.11</b>	<b>31.56</b>	<b>.00</b>	<b>.44</b>	<b>12.65</b>	<b>.00</b>	<b>.24</b>	

$p$  Values are uncorrected; **bold** print denotes significant tests after FDR correction.

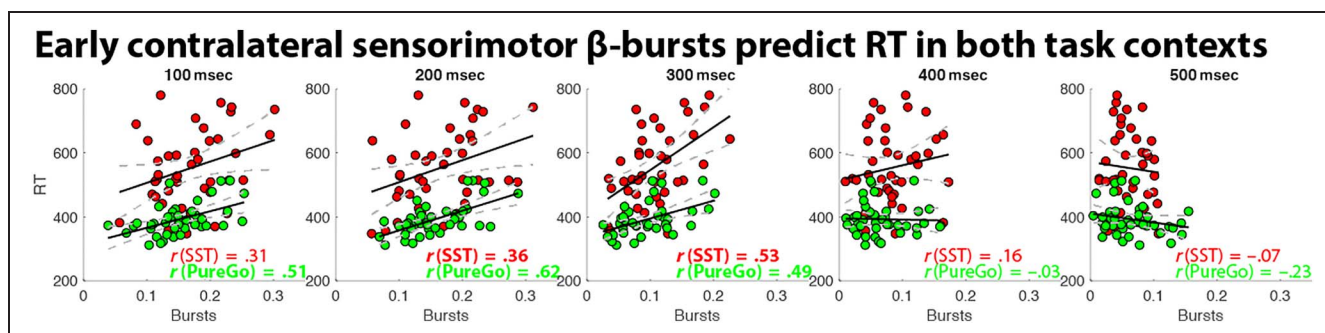


**Figure 4.** Brain–behavior correlations between go-trial RT and contralateral sensorimotor  $\beta$ -bursts in both task contexts. Across both tasks, early levels of  $\beta$ -bursting positively predicted RT, with increased bursting leading to slower RTs. Values in **bold** print were significant after FDR correction to a family-wise  $p = .05$  (see Table 2 for exact  $p$  values).

sensorimotor  $\beta$ -bursts and basic RT that is not specific to whether proactive inhibitory control is present. After FDR correction, positive correlations were observable between  $\beta$ -bursts and go-trial RT in Bins 2 and 3 for stop-signal blocks and in Bins 1–3 for pure-go blocks (Figure 4 and Table 2).

### Brain–Behavior Correlations: Context-dependent $\beta$ -Burst Increase vs. Proactive RT Slowing

In line with the main hypothesis of the current study, there was also a significantly positive relationship between the degree of increase in sensorimotor  $\beta$ -burst rate each participant showed in the stop-signal compared to the pure-go context and the degree to which they slowed their responses in the stop-signal context (Figure 5). Notably, this was only true for the contralateral  $\beta$ -bursts ( $r = .33$ ,  $p < .05$ ), whereas the ipsilateral  $\beta$ -bursts did not show the same relationship ( $r = .03$ ,  $p = .84$ ).

### Exploratory Analysis: Pre-go Baseline

In addition to the  $\beta$ -burst rates that occurred in the movement initiation period after the go-signal (the investigation

of which was motivated by our previous study; Wessel, 2020), we also explored whether potential differences in  $\beta$ -burst rates between the stop- and pure-go contexts were already present before the go-signal. This would indicate that proactive control is tonically deployed throughout the task, whereas a null finding would indicate that proactive control is deployed in a more transient, phasic fashion during movement initiation itself. In line with the former interpretation, prestimulus sensorimotor  $\beta$ -burst rate in stop-blocks was 0.181 bursts per 100 msec ( $SD = 0.049$ ), whereas the same period in pure-go blocks showed a rate of 0.171 bursts per 100 msec ( $SD = 0.046$ ,  $t(40) = 3.1$ ,  $p = .0036$ ,  $d = 0.22$ ). This shows that sensorimotor  $\beta$ -bursting was increased even before the to-be-initiated movement was known or cued. However, unlike burst rates in the movement initiation period (Figure 5), this pre-go baseline increase in sensorimotor  $\beta$ -bursts was not related to behavior in the form of proactive RT slowing ( $r = .06$ ,  $p = .7$ ). This suggests that, although  $\beta$  is increased even before the movement is known, this increase only becomes effective in influencing behavior once an actual movement has been cued and is initiated.

### Exploratory Analysis: Multivariate Pattern Analysis of the Pre-go Baseline Period

To confirm the abovementioned exploratory finding of increased sensorimotor  $\beta$ -bursting during the prestimulus baseline period in stop-signal blocks, we attempted to replicate the finding using a complete different analysis approach. Specifically, we explored if the task context (stop or pure-go) could be decoded from the whole-scalp  $\beta$ -band activity even before go-stimulus onset (i.e., during the baseline). These analyses were performed using the multivariate pattern analysis (MVPA) method implemented in the ADAM toolbox (Fahrenfort, Van Driel, Van Gaal, & Olivers, 2018).

To this end, we used the same data as for the abovementioned  $\beta$ -burst analysis (i.e., the CSD-transformed and cleaned data on which the burst detection was performed) and epoched the  $\beta$ -band amplitude signal for each trial (15–29 Hz, extracted using the seven-cycle Morlet wavelet

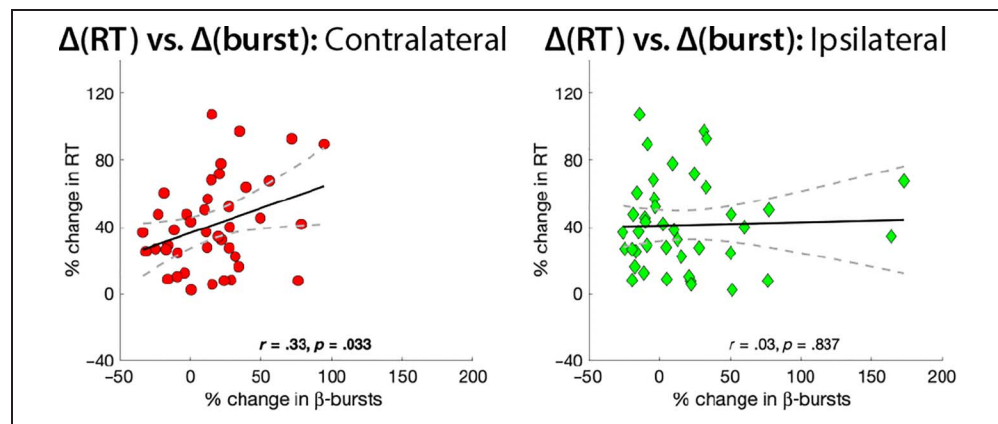
**Table 2.** Test Statistics for Bin-Wise Correlations between Contralateral Sensorimotor  $\beta$ -Bursts and Go-Trial RT Across Both Task Contexts

Bin		Context			
		Stop-Signal		Pure-go	
		<i>r</i>	<i>p</i>	<i>r</i>	<i>p</i>
0–100	.310	.045	<b>.505</b>	<b>.001</b>	
100–200	<b>.364</b>	<b>.019</b>	<b>.620</b>	<b>.000</b>	
200–300	<b>.532</b>	<b>.000</b>	<b>.494</b>	<b>.001</b>	
300–400	.161	.314	-.032	.844	
400–500	-.071	.659	-.226	.155	

**Bold** print signifies significant tests after FDR correction to a family-wise  $p < .05$ .



**Figure 5.** Correlation between the change in early  $\beta$ -bursting between both task contexts (during the bins that showed a significant increase in average burst rate after FDR correction; cf. Figure 3) and proactive RT slowing across participants, separately for contralateral and ipsilateral electrode sites.



described above) from  $-500$  to  $500$  msec around the go-stimulus. To avoid biasing the classifier, trial counts were equated across both conditions by removing a random selection of trials from the condition with more exemplars. To train and test the classifier, we used linear discriminant analysis (Grootswagers, Wardle, & Carlson, 2017) on the single-trial data for each participant, with the quality of the classification evaluated with leave-one-out cross-validation. We then quantified the area under the resultant receiver operating characteristic curve (i.e., the cumulative probability of correct classification plotted against the cumulative probability of false-positive classification) for this validation procedure. Each participant's resulting vector of area under the resultant receiver operating characteristic curve data at each time point was then submitted to sample point-wise paired-samples  $t$  test against chance (.5), corrected for multiple comparisons using cluster-based permutation testing (Maris & Oostenveld, 2007; 10,000 iterations, cluster  $p$  value = .05, alpha = .001).

Confirming the findings from the  $\beta$ -burst analysis, the MVPA showed that the task condition could indeed be successfully decoded from  $\beta$  activity. In the post-go period, decoding accuracy notably increased in the later periods,

which likely reflects the earlier occurrence of postmovement  $\beta$  rebound (Jurkiewicz, Gaetz, Bostan, & Cheyne, 2006; Pfurtscheller, Neuper, Brunner, & Da Silva, 2005) in the pure-go condition (which contained faster responses on average). Notably, however, in line with the exploratory  $\beta$ -burst analysis, classification was already above chance during the pre-go baseline period (Figure 6). Moreover, the topography of the forward-reconstructed weight matrix reveals that most of the contribution to decoding performance came from sensorimotor sites. This confirms the analysis from the exploratory burst analysis.

Furthermore, identical analyses of theta ( $5\text{--}8$  Hz) and alpha ( $9\text{--}12$  Hz) activity showed that neither frequency band showed above-chance decoding in the pre-go baseline period, underscoring that  $\beta$ -band activity in the baseline period is uniquely related to proactive control.

### Exploratory Analysis: Baseline-Normalized Post-go $\beta$ -Burst Changes

Following up on the finding that differences in sensorimotor  $\beta$ -burst rates were already present in the prestimulus baseline period, we also reinvestigated the post-go data.

**Figure 6.** Using whole-scalp  $\beta$ -band ( $15\text{--}29$  Hz) data to decode task conditions using MVPA. Confirming the results from both the hypothesis-driven analysis of the post-go  $\beta$ -band burst data and the exploratory analysis of the pre-go baseline period, task context (stop vs. pure-go) could be successfully decoded from  $\beta$ -band data in both periods. Moreover, forward-reconstructed decoding weight matrices at the significant clusters in both time ranges show that most explanatory power was provided by activity over bilateral sensorimotor sites.

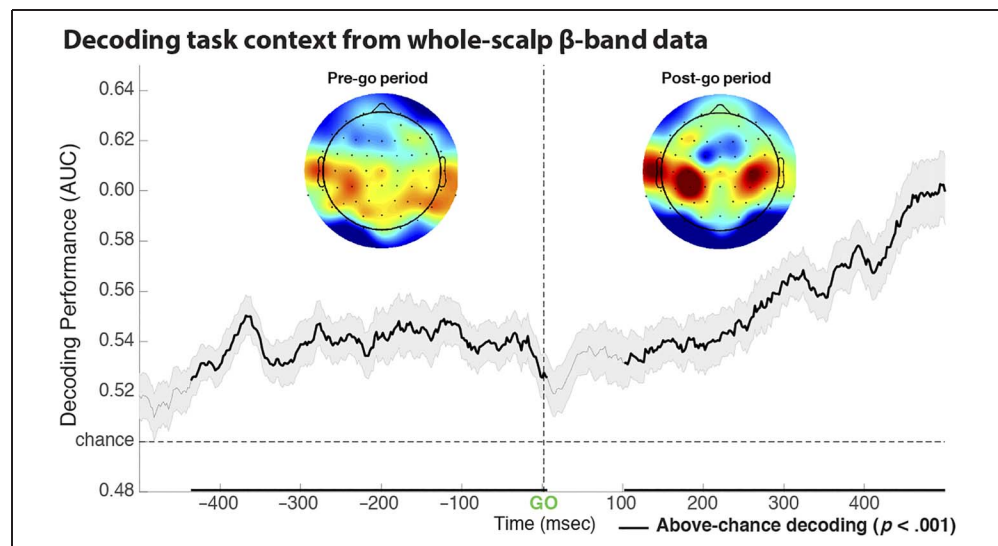


**Table 3.** Test Statistics for Bin-Wise ANOVAs of Sensorimotor  $\beta$ -Bursts After Go-Signals, Normalized by Baseline (cf. Figure 5)

Bin		Variable								
		Context			Laterality			Interaction		
		<i>F</i>	<i>p</i>	$\eta^2$	<i>F</i>	<i>p</i>	$\eta^2$	<i>F</i>	<i>p</i>	$\eta^2$
0–100	0.42	.52	.01	0.17	.68	.00	0.69	.41	.02	
100–200	0.11	.74	.00	0.25	.62	.01	0.24	.63	.01	
200–300	2.59	.12	.06	2.33	.13	.06	0.40	.53	.01	
300–400	0.91	.35	.02	<b>15.49</b>	<b>.00</b>	.28	0.69	.41	.02	
400–500	0.41	.52	.01	<b>26.28</b>	<b>.00</b>	.40	<b>9.81</b>	<b>.00</b>	<b>.20</b>	

*p* Values are uncorrected; **bold** print denotes significant tests after FDR correction.

In particular, instead of investigating raw burst counts, we reran the same analyses performed in the main hypothesis test, but normalizing each bin and condition by the appropriate baseline burst rate (i.e., contralateral post-go activity for a left-hand response trial in the stopping condition was normalized by the mean baseline burst rate in the stopping condition at electrode C4, and so forth). This revealed that, although the late-period effects of laterality (in the 300- to 400-msec and 400- to 500-msec windows) and the interaction in the final bin (400–500 msec) remained significant, none of the five post-go bins retained any significant burst rate differences between the two task contexts (i.e., between stop and pure-go blocks). The exact statistics for each bin can be found in Table 3, and the data are visualized in Figure 7.

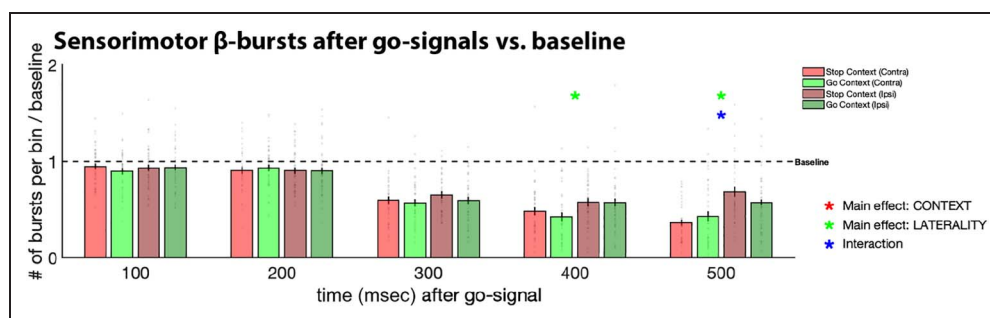
What this shows is that the post-go differences in raw burst rates (Figure 1) can be, at least to a substantial degree, attributed to condition differences that are already present in the baseline burst rates. In other words, it appears that broad, nonselective inhibitory control in the absence of foreknowledge is implemented by a global increase of  $\beta$ -bursting both before and after a signal to initiate a movement. Notably, the main brain–behavior analysis in the hypothesis-testing part of this study showed that the contralateral  $\beta$ -burst rate difference in the post-go period did predict proactive RT slowing—that is, the behavioral expression of proactive inhibition (this association

remained significant when the data were corrected for baseline differences as well;  $r = .35$ ,  $p = .027$ ). Importantly, as noted above, this was not the case for the burst-rate condition differences in the pre-go baseline period.

## DISCUSSION

$\beta$ -Band activity is a fundamental neurophysiological signature of the motor system. Our current study shows that, when human participants strategically implement proactive inhibitory motor control in anticipation of potentially having to stop a movement,  $\beta$ -burst rates over bilateral sensorimotor cortex were increased. Further analyses showed that this relative increase was already present in the baseline period—that is, before the movement in question was known or cued. Indeed, this was further underscored by MVPAs that demonstrated that the task condition (and the associated engagement of proactive control) could already be successfully decoded from  $\beta$ -band activity that occurred before any signal to initiate a response (i.e., before the go-signal). Brain–behavior correlation analyses then revealed that this tonic increase in sensorimotor  $\beta$ -bursting throughout the task period affected behavior specifically during the movement initiation period: Participants with greater relative increases in sensorimotor  $\beta$ -bursting

**Figure 7.** Baseline-normalized version of Figure 3. Sensorimotor  $\beta$ -bursts in five consecutive time bins after go-signals in both task contexts, separately for contralateral (Contra) and ipsilateral (Ipsi) electrode sites. Gray dots represent individual participant means; black bars denote the standard error of the group mean. Asterisks denote significance of the respective main effect or interaction within the specified bin, corrected for multiple comparisons using FDR to a family-wise  $p < .05$ .



between the two task contexts also showed greater proactive RT slowing.

The current data have several notable features. First, independent of whether proactive control was engaged or not, sensorimotor  $\beta$ -burst rates during movement initiation predicted RTs in both task contexts (Figure 4). This confirms that  $\beta$ -bursts may reflect a general signature of a net-inhibited motor system, which has to be overcome to initiate a movement (Pfurtscheller et al., 1997). Moreover, it speaks toward recent conceptualizations of motor inhibition as a generic, universal mechanism that is involved in movement planning, with the degree of its deployment depending on—among other things—proactive control settings (Raud et al., 2020; Greenhouse, Sias, Labruna, & Ivry, 2015). Second, adjustments to proactive inhibitory control resulted in an increase of sensorimotor burst rates both before and after a signal to initiate a movement. This shows that humans adjust the overall, general inhibition of their corticomotor system when they anticipate that they may have to stop an action after its initiation, even when they have no foreknowledge of the specific movement that they may have to stop. Although this bilateral increase in net inhibition of the motor system is already observable before the go-signal even appeared, it does appear to be specifically implemented in service of inhibiting behavior during the movement initiation period (which is when it becomes predictive of condition-related increases in proactive RT slowing). Moreover, whereas the overall increase in  $\beta$  activity was observed bilaterally, the predictive relationship between  $\beta$  and RT was specific to contralateral  $\beta$  increases. Hence, humans appear to nonselectively deploy proactive inhibitory control as a broad task setting—both during and before movement initiation, and both at contralateral and ipsilateral motor sites—but with the goal of achieving a site-specific inhibition of the to-be-performed movement specifically during its initiation. Third, the pre-go baseline increase in sensorimotor  $\beta$ -burst rates suggests that, in the absence of foreknowledge, humans implement proactive inhibitory control via a sustained increase of sensorimotor  $\beta$ -bursting, instead of a transient engagement of  $\beta$ -bursting that is specific to the movement initiation period. A highly notable implication of this finding is that studies that seek to identify the cognitive control signatures that produce the ultimate effect of increased sensorimotor  $\beta$ -bursting observed here should avoid baseline-corrected contrasts of post-go activity. Instead, potential condition differences in the upstream processes should be investigated as sustained differences that are likely present throughout most (or all) of the respective task periods, not just during movement initiation.

The current study shows that proactive inhibitory control in the context of the SST is implemented at the level of the motor system by sustaining the inhibited state of the sensorimotor cortex past the signal to initiate an action. In other words, if a movement is executed under an increased amount of caution, the corticomotor system remains inhibited for an extended period. This is in line

with existing literature that used TMS to probe the net excitability of entire corticospinal tracts during stop-signal-type tasks (Duque et al., 2017; Cowie, MacDonald, Cirillo, & Byblow, 2016; Greenhouse et al., 2011; Claffey et al., 2010). Specifically, these studies show that the implementation of proactive motor inhibition directly affects the motor system and is not solely attributable to attentional processes that aid stop-signal detection. Whereas most of these studies have shown that this is the case when participants have specific foreknowledge of the to-be-inhibited response, the current results show that this is also true when the to-be-inhibited response is unknown ahead of time. More generally, these findings support the view that sensorimotor  $\beta$ -band activity reflects an inhibited state of the motor system (Schulz et al., 2013; Zhang et al., 2008; Pfurtscheller et al., 1997).

Notably, motor caution is an executive function that is implemented in many controlled behaviors that occur even outside SSTs. Indeed, increases in motor threshold are purported to underlie more cautious, controlled responding in a slew of cognitive control scenarios that are subject to scientific study, including error commission (Fischer, Nigbur, Klein, Danielmeier, & Ullsperger, 2018; Ullsperger & Danielmeier, 2016; Ridderinkhof, 2002; Ridderinkhof et al., 2002), response conflict (Wessel, Waller, & Greenlee, 2019; Klein, Petitjean, Olivier, & Duque, 2014; Burle, Possamai, Vidal, Bonnet, & Hasbroucq, 2002; Botvinick, Braver, Barch, Carter, & Cohen, 2001), task switching (Mansfield, Karayanidis, Jamaadar, Heathcote, & Forstmann, 2011), and decision conflict (Cavanagh et al., 2011; Frank, 2006). It is tempting to assume that a global, bilateral increase of sensorimotor  $\beta$  activity could reflect an increase in overall response threshold, implemented via a broad recruitment of proactive inhibitory control. Indeed, along those lines, some studies have recently connected sensorimotor  $\beta$ -band activity to adjustments in response thresholds in situations that demand cognitive control, even outside explicit stop-signal scenarios (e.g., Fischer et al., 2018; Tan, Wade, & Brown, 2016). The potential universality of this signature outside the SST and its direct relationship to the inhibition of the motor system therefore yields a promising avenue for future study.

On the methodological side, the current study provides another demonstration of the recent development toward investigating sensorimotor  $\beta$ -band activity as rate-modulated burst-like activity, rather than as amplitude-modulated oscillations (e.g., Wessel, 2020; Shin et al., 2017; Sherman et al., 2016; Feingold et al., 2015), a notion for which there is now converging evidence from both the rodent and primate literature (both in the human and nonhuman realms). In our previous investigation of the SST, we have found that burst quantifications can reveal brain–behavior correlations that are absent when quantifying the signal in a classic amplitude-modulated fashion (Wessel, 2020). Indeed, the clarity of the brain–behavior relationships in the current study (both in terms of simple RT and even in terms of strategic changes in RT across two different task contexts)

suggests that even noninvasive scalp recordings can, without any additional preprocessing or specific spatial filters, provide sufficient power to investigate movement-related brain activity, if  $\beta$  is investigated using a burst-based quantification. Moreover, there is a growing body of recent human clinical literature suggesting that even subcortical  $\beta$  activity (e.g., in the BG) may be better characterized by short, transient bursts, whose features index specific motor-related symptoms in populations with movement disorders (Little, Bonaiuto, Barnes, & Bestmann, 2019; Anidi et al., 2018; Tinkhauser et al., 2017). Given that both proactive and reactive control deficits are well-known symptoms of such disorders (Benis et al., 2014; Obeso et al., 2013, 2014; van den Wildenberg et al., 2006), burst-based quantifications of  $\beta$ -band activity from both invasive and noninvasive recordings yield a tremendous potential for future clinical investigations of abnormalities in inhibitory control and their neurophysiological basis.

In summary, the current study provides strong evidence for the fact that sensorimotor  $\beta$ -bursting is a general signature of an inhibited motor system, which can be globally upregulated to implement inhibitory motor control, even when the specific motor effector to be inhibited is not known ahead of time. The results also provide further evidence for the view that proactive inhibitory control is achieved via direct effects on the motor system and against the view that proactive control is solely achieved by attentional tuning.

Reprint requests should be sent to Jan R. Wessel or Cheol Soh, Department of Psychological and Brain Sciences, University of Iowa, 444 MRC, Iowa City, IA 52242, or via e-mail: Jan-Wessel@uiowa.edu, Cheol-Soh@uiowa.edu.

### Author Contributions

Cheol Soh: Conceptualization; Formal analysis; Investigation; Visualization; Writing—Review & editing. Megan Hynd: Investigation; Writing—Review & editing. Benjamin Rangel: Investigation; Writing—Review & editing. Jan Wessel: Conceptualization; Funding acquisition; Investigation; Project administration; Supervision; Visualization; Writing—Original draft; Writing—Review & editing.

### Funding Information

National Institute of Neurological Disorders and Stroke (<http://dx.doi.org/10.13039/1000000065>), grant number: R01 NS117753. National Science Foundation (<http://dx.doi.org/10.13039/1000000001>), grant number: CAREER 1752355.

### Diversity in Citation Practices

A retrospective analysis of the citations in every article published in this journal from 2010 to 2020 has revealed a persistent pattern of gender imbalance: Although the

proportions of authorship teams (categorized by estimated gender identification of first author/last author) publishing in the *Journal of Cognitive Neuroscience (JoCN)* during this period were  $M(an)/M = .408$ ,  $W(oman)/M = .335$ ,  $M/W = .108$ , and  $W/W = .149$ , the comparable proportions for the articles that these authorship teams cited were  $M/M = .579$ ,  $W/M = .243$ ,  $M/W = .102$ , and  $W/W = .076$  (Fulvio et al., *JoCN*, 33:1, pp. 3–7). Consequently, *JoCN* encourages all authors to consider gender balance explicitly when selecting which articles to cite and gives them the opportunity to report their article's gender citation balance.

### REFERENCES

- Anidi, C., O'Day, J. J., Anderson, R. W., Afzal, M. F., Syrkin-Nikolau, J., Velisar, A., et al. (2018). Neuromodulation targets pathological not physiological  $\beta$  bursts during gait in Parkinson's disease. *Neurobiology of Disease*, 120, 107–117. DOI: <https://doi.org/10.1016/j.nbd.2018.09.004>, PMID: 30196050, PMCID: PMC6422345
- Aron, A. R. (2011). From reactive to proactive and selective control: Developing a richer model for stopping inappropriate responses. *Biological Psychiatry*, 69, e55–e68. DOI: <https://doi.org/10.1016/j.biopsych.2010.07.024>, PMID: 20932513, PMCID: PMC3039712
- Aron, A. R., Robbins, T. W., & Poldrack, R. A. (2014). Inhibition and the right inferior frontal cortex: One decade on. *Trends in Cognitive Sciences*, 18, 177–185. DOI: <https://doi.org/10.1016/j.tics.2013.12.003>, PMID: 24440116
- Baker, S. N. (2007). Oscillatory interactions between sensorimotor cortex and the periphery. *Current Opinion in Neurobiology*, 17, 649–655. DOI: <https://doi.org/10.1016/j.conb.2008.01.007>, PMID: 18339546, PMCID: PMC2428102
- Bell, A. J., & Sejnowski, T. J. (1995). An information-maximization approach to blind separation and blind deconvolution. *Neural Computation*, 7, 1129–1159. DOI: <https://doi.org/10.1162/neco.1995.7.6.1129>, PMID: 7584893
- Benis, D., David, O., Lachaux, J.-P., Seigneuret, E., Krack, P., Fraix, V., et al. (2014). Subthalamic nucleus activity dissociates proactive and reactive inhibition in patients with Parkinson's disease. *Neuroimage*, 91, 273–281. DOI: <https://doi.org/10.1016/j.neuroimage.2013.10.070>, PMID: 24368260
- Benjamini, Y., Krieger, A. M., & Yekutieli, D. (2006). Adaptive linear step-up procedures that control the false discovery rate. *Biometrika*, 93, 491–507. DOI: <https://doi.org/10.1093/biomet/93.3.491>
- Botvinick, M. M., Braver, T. S., Barch, D. M., Carter, C. S., & Cohen, J. D. (2001). Conflict monitoring and cognitive control. *Psychological Review*, 108, 624–652. DOI: <https://doi.org/10.1037/0033-295X.108.3.624>, PMID: 11488380
- Brainard, D. H. (1997). The psychophysics toolbox. *Spatial Vision*, 10, 433–436. DOI: <https://doi.org/10.1163/156856897X00357>
- Braver, T. S. (2012). The variable nature of cognitive control: A dual mechanisms framework. *Trends in Cognitive Sciences*, 16, 106–113. DOI: <https://doi.org/10.1016/j.tics.2011.12.010>, PMID: 22245618, PMCID: PMC3289517
- Burle, B., Possamaï, C.-A., Vidal, F., Bonnet, M., & Hasbroucq, T. (2002). Executive control in the Simon effect: An electromyographic and distributional analysis. *Psychological Research*, 66, 324–336. DOI: <https://doi.org/10.1007/s00426-002-0105-6>, PMID: 12466929
- Cai, W., Chen, T., Ide, J. S., Li, C.-S. R., & Menon, V. (2016). Dissociable fronto-operculum-insula control signals for anticipation and detection of inhibitory sensory cue. *Cerebral*

- Cortex*, 27, 4073–4082. DOI: <https://doi.org/10.1093/cercor/bhw219>, PMID: 27473319, PMCID: PMC6059112
- Cai, W., George, J. S., Verbruggen, F., Chambers, C. D., & Aron, A. R. (2012). The role of the right presupplementary motor area in stopping action: Two studies with event-related transcranial magnetic stimulation. *Journal of Neurophysiology*, 108, 380–389. DOI: <https://doi.org/10.1152/jn.00132.2012>, PMID: 22514296, PMCID: PMC3404792
- Cai, Y., Li, S., Liu, J., Li, D., Feng, Z., Wang, Q., et al. (2015). The role of the frontal and parietal cortex in proactive and reactive inhibitory control: A transcranial direct current stimulation study. *Journal of Cognitive Neuroscience*, 28, 177–186. DOI: [https://doi.org/10.1162/jocn\\_a\\_00888](https://doi.org/10.1162/jocn_a_00888), PMID: 26439269
- Cavanagh, J. F., Wiecki, T. V., Cohen, M. X., Figueroa, C. M., Samanta, J., Sherman, S. J., et al. (2011). Subthalamic nucleus stimulation reverses mediofrontal influence over decision threshold. *Nature Neuroscience*, 14, 1462–1467. DOI: <https://doi.org/10.1038/nn.2925>, PMID: 21946325, PMCID: PMC3394226
- Chikazoe, J., Jimura, K., Hirose, S., Yamashita, K.-I., Miyashita, Y., & Konishi, S. (2009). Preparation to inhibit a response complements response inhibition during performance of a stop-signal task. *Journal of Neuroscience*, 29, 15870–15877. DOI: <https://doi.org/10.1523/JNEUROSCI.3645-09.2009>, PMID: 20016103, PMCID: PMC6666181
- Claffey, M. P., Sheldon, S., Stinear, C. M., Verbruggen, F., & Aron, A. R. (2010). Having a goal to stop action is associated with advance control of specific motor representations. *Neuropsychologia*, 48, 541–548. DOI: <https://doi.org/10.1016/j.neuropsychologia.2009.10.015>, PMID: 19879283, PMCID: PMC2813913
- Cowie, M. J., MacDonald, H. J., Cirillo, J., & Byblow, W. D. (2016). Proactive modulation of long-interval intracortical inhibition during response inhibition. *Journal of Neurophysiology*, 116, 859–867. DOI: <https://doi.org/10.1152/jn.00144.2016>, PMID: 27281744, PMCID: PMC4995280
- Cunillera, T., Brignani, D., Cucurell, D., Fuentemilla, L., & Miniussi, C. (2016). The right inferior frontal cortex in response inhibition: A tDCS–ERP co-registration study. *Neuroimage*, 140, 66–75. DOI: <https://doi.org/10.1016/j.neuroimage.2015.11.044>, PMID: 26619787
- Cunillera, T., Fuentemilla, L., Brignani, D., Cucurell, D., & Miniussi, C. (2014). A simultaneous modulation of reactive and proactive inhibition processes by anodal tDCS on the right inferior frontal cortex. *PLoS One*, 9, e113537. DOI: <https://doi.org/10.1371/journal.pone.0113537>, PMID: 25426713, PMCID: PMC4245139
- Delorme, A., & Makeig, S. (2004). EEGLAB: An open source toolbox for analysis of single-trial EEG dynamics including independent component analysis. *Journal of Neuroscience Methods*, 134, 9–21. DOI: <https://doi.org/10.1016/j.jneumeth.2003.10.009>, PMID: 15102499
- Delorme, A., Palmer, J., Onton, J., Oostenveld, R., & Makeig, S. (2012). Independent EEG sources are dipolar. *PLoS One*, 7, e30135. DOI: <https://doi.org/10.1371/journal.pone.0030135>, PMID: 22355308, PMCID: PMC3280242
- Delorme, A., Sejnowski, T., & Makeig, S. (2007). Enhanced detection of artifacts in EEG data using higher-order statistics and independent component analysis. *Neuroimage*, 34, 1443–1449. DOI: <https://doi.org/10.1016/j.neuroimage.2006.11.004>, PMID: 17188898, PMCID: PMC2895624
- Duque, J., Greenhouse, I., Labruna, L., & Ivry, R. B. (2017). Physiological markers of motor inhibition during human behavior. *Trends in Neurosciences*, 40, 219–236. DOI: <https://doi.org/10.1016/j.tins.2017.02.006>, PMID: 28341235, PMCID: PMC5389740
- Elchlepp, H., Lavric, A., Chambers, C. D., & Verbruggen, F. (2016). Proactive inhibitory control: A general biasing account. *Cognitive Psychology*, 86, 27–61. DOI: <https://doi.org/10.1016/j.cogpsych.2016.01.004>, PMID: 26859519, PMCID: PMC4825542
- Engel, A. K., & Fries, P. (2010).  $\beta$ -band oscillations—Signalling the status quo? *Current Opinion in Neurobiology*, 20, 156–165. DOI: <https://doi.org/10.1016/j.conb.2010.02.015>, PMID: 20359884
- Fahrenfort, J. J., Van Driel, J., Van Gaal, S., & Olivers, C. N. (2018). From ERPs to MVPA using the Amsterdam decoding and modeling toolbox (ADAM). *Frontiers in Neuroscience*, 12, 368. DOI: <https://doi.org/10.3389/fnins.2018.00368>, PMID: 30018529, PMCID: PMC6038716
- Feingold, J., Gibson, D. J., DePasquale, B., & Graybiel, A. M. (2015). Bursts of  $\beta$  oscillation differentiate postperformance activity in the striatum and motor cortex of monkeys performing movement tasks. *Proceedings of the National Academy of Sciences, U.S.A.*, 112, 13687–13692. DOI: <https://doi.org/10.1073/pnas.1517629112>, PMID: 26460033, PMCID: PMC4640760
- Fischer, A. G., Nigbur, R., Klein, T. A., Danielmeier, C., & Ullsperger, M. (2018). Cortical  $\beta$  power reflects decision dynamics and uncovers multiple facets of post-error adaptation. *Nature Communications*, 9, 5038. DOI: <https://doi.org/10.1038/s41467-018-07456-8>, PMID: 30487572, PMCID: PMC6261941
- Frank, M. J. (2006). Hold your horses: A dynamic computational role for the subthalamic nucleus in decision making. *Neural Networks*, 19, 1120–1136. DOI: <https://doi.org/10.1016/j.neunet.2006.03.006>, PMID: 16945502
- Greenhouse, I., Oldenkamp, C. L., & Aron, A. R. (2011). Stopping a response has global or nonglobal effects on the motor system depending on preparation. *Journal of Neurophysiology*, 107, 384–392. DOI: <https://doi.org/10.1152/jn.00704.2011>, PMID: 22013239, PMCID: PMC3349702
- Greenhouse, I., Sias, A., Labruna, L., & Ivry, R. B. (2015). Nonspecific inhibition of the motor system during response preparation. *Journal of Neuroscience*, 35, 10675–10684. DOI: <https://doi.org/10.1523/JNEUROSCI.1436-15.2015>, PMID: 26224853, PMCID: PMC4518047
- Greenhouse, I., & Wessel, J. R. (2013). EEG signatures associated with stopping are sensitive to preparation. *Psychophysiology*, 50, 900–908. DOI: <https://doi.org/10.1111/psyp.12070>, PMID: 23763667, PMCID: PMC3745550
- Grootswagers, T., Wardle, S. G., & Carlson, T. A. (2017). Decoding dynamic brain patterns from evoked responses: A tutorial on multivariate pattern analysis applied to time series neuroimaging data. *Journal of Cognitive Neuroscience*, 29, 677–697. DOI: [https://doi.org/10.1162/jocn\\_a\\_01068](https://doi.org/10.1162/jocn_a_01068), PMID: 27779910
- Hynd, M., Soh, C., Rangel, B. O., & Wessel, J. R. (2021). Paired-pulse TMS and scalp EEG reveal systematic relationship between inhibitory GABA<sub>A</sub> signaling in M1 and fronto-central cortical activity during action stopping. *Journal of Neural Physiology*, 125, 648–660. DOI: <https://doi.org/10.1152/jn.00571.2020>
- Jaffard, M., Longcamp, M., Velay, J.-L., Anton, J.-L., Roth, M., Nazarian, B., et al. (2008). Proactive inhibitory control of movement assessed by event-related fMRI. *Neuroimage*, 42, 1196–1206. DOI: <https://doi.org/10.1016/j.neuroimage.2008.05.041>, PMID: 18588986
- Jahanshahi, M., Obeso, I., Rothwell, J. C., & Obeso, J. A. (2015). A fronto–striato–subthalamic–pallidal network for goal-directed and habitual inhibition. *Nature Reviews Neuroscience*, 16, 719–732. DOI: <https://doi.org/10.1038/nrn4038>, PMID: 26530468
- Jahfari, S., Stinear, C. M., Claffey, M., Verbruggen, F., & Aron, A. R. (2009). Responding with restraint: What are the neurocognitive mechanisms? *Journal of Cognitive Neuroscience*, 22, 1479–1492. DOI: <https://doi.org/10.1162/jocn.2009.21307>, PMID: 19583473, PMCID: PMC2952035
- Jurkiewicz, M. T., Gaetz, W. C., Bostan, A. C., & Cheyne, D. (2006). Post-movement beta rebound is generated in motor

- cortex: Evidence from neuromagnetic recordings. *Neuroimage*, 32, 1281–1289. **DOI:** <https://doi.org/10.1016/j.neuroimage.2006.06.005>, **PMID:** 16863693
- Kenemans, J. L. (2015). Specific proactive and generic reactive inhibition. *Neuroscience & Biobehavioral Reviews*, 56, 115–126. **DOI:** <https://doi.org/10.1016/j.neubiorev.2015.06.011>, **PMID:** 26116545
- Kilavik, B. E., Zaepffel, M., Brovelli, A., MacKay, W. A., & Riehle, A. (2013). The ups and downs of  $\beta$  oscillations in sensorimotor cortex. *Experimental Neurology*, 245, 15–26. **DOI:** <https://doi.org/10.1016/j.expneurol.2012.09.014>, **PMID:** 23022918
- Klein, P.-A., Petitjean, C., Olivier, E., & Duque, J. (2014). Top-down suppression of incompatible motor activations during response selection under conflict. *Neuroimage*, 86, 138–149. **DOI:** <https://doi.org/10.1016/j.neuroimage.2013.08.005>, **PMID:** 23939021
- Lee, T. W., Girolami, M., & Sejnowski, T. J. (1999). Independent component analysis using an extended infomax algorithm for mixed subgaussian and supergaussian sources. *Neural Computation*, 11, 417–441. **DOI:** <https://doi.org/10.1162/089976699300016719>, **PMID:** 9950738
- Little, S., Bonaiuto, J., Barnes, G., & Bestmann, S. (2019). Human motor cortical  $\beta$  bursts relate to movement planning and response errors. *PLoS Biology*, 17, e3000479. **DOI:** <https://doi.org/10.1371/journal.pbio.3000479>, **PMID:** 31584933, **PMCID:** PMC6795457
- Logan, G. D., Cowan, W. B., & Davis, K. A. (1984). On the ability to inhibit simple and choice reaction time responses: A model and a method. *Journal of Experimental Psychology: Human Perception and Performance*, 10, 276–291. **DOI:** <https://doi.org/10.1037/0096-1523.10.2.276>
- Majid, D. S. A., Cai, W., Corey-Bloom, J., & Aron, A. R. (2013). Proactive selective response suppression is implemented via the basal ganglia. *Journal of Neuroscience*, 33, 13259–13269. **DOI:** <https://doi.org/10.1523/JNEUROSCI.5651-12.2013>, **PMID:** 23946385, **PMCID:** PMC3742918
- Majid, D. S. A., Cai, W., George, J. S., Verbruggen, F., & Aron, A. R. (2011). Transcranial magnetic stimulation reveals dissociable mechanisms for global versus selective corticomotor suppression underlying the stopping of action. *Cerebral Cortex*, 22, 363–371. **DOI:** <https://doi.org/10.1093/cercor/bhr112>, **PMID:** 21666129, **PMCID:** PMC3256406
- Mansfield, E. L., Karayanidis, F., Jamadar, S., Heathcote, A., & Forstmann, B. U. (2011). Adjustments of response threshold during task switching: A model-based functional magnetic resonance imaging study. *Journal of Neuroscience*, 31, 14688–14692. **DOI:** <https://doi.org/10.1523/JNEUROSCI.2390-11.2011>, **PMID:** 21994385, **PMCID:** PMC6703389
- Maris, E., & Oostenveld, R. (2007). Nonparametric statistical testing of EEG- and MEG-data. *Journal of Neuroscience Methods*, 164, 177–190. **DOI:** <https://doi.org/10.1016/j.jneumeth.2007.03.024>, **PMID:** 17517438
- McFarland, D. J., Miner, L. A., Vaughan, T. M., & Wolpaw, J. R. (2000). Mu and beta rhythm topographies during motor imagery and actual movements. *Brain Topography*, 12, 177–186. **DOI:** <https://doi.org/10.1023/A:1023437823106>, **PMID:** 10791681
- Meyer, H. C., & Bucci, D. J. (2016). Neural and behavioral mechanisms of proactive and reactive inhibition. *Learning & Memory*, 23, 504–514. **DOI:** <https://doi.org/10.1101/lm.040501.115>, **PMID:** 27634142, **PMCID:** PMC5026209
- Muralidharan, V., Yu, X., Cohen, M. X., & Aron, A. R. (2019). Preparing to stop action increases  $\beta$  band power in contralateral sensorimotor cortex. *Journal of Cognitive Neuroscience*, 31, 657–668. **DOI:** [https://doi.org/10.1162/jocn\\_a\\_01373](https://doi.org/10.1162/jocn_a_01373), **PMID:** 30633601
- Neuper, C., Wörtz, M., & Pfurtscheller, G. (2006). ERD/ERS patterns reflecting sensorimotor activation and deactivation. In C. Neuper & W. Klimesch (Eds.), *Progress in brain research* (pp. 211–222). Elsevier. **DOI:** [https://doi.org/10.1016/S0079-6123\(06\)59014-4](https://doi.org/10.1016/S0079-6123(06)59014-4)
- Obeso, I., Cho, S. S., Antonelli, F., Houle, S., Jahanshahi, M., Ko, J. H., et al. (2013). Stimulation of the pre-SMA influences cerebral blood flow in frontal areas involved with inhibitory control of action. *Brain Stimulation*, 6, 769–776. **DOI:** <https://doi.org/10.1016/j.brs.2013.02.002>, **PMID:** 23545472
- Obeso, I., Wilkinson, L., Casabona, E., Speekenbrink, M., Luisa Bringas, M., Álvarez, M., et al. (2014). The subthalamic nucleus and inhibitory control: Impact of subthalamotomy in Parkinson's disease. *Brain*, 137, 1470–1480. **DOI:** <https://doi.org/10.1093/brain/awu058>, **PMID:** 24657985
- Perrin, F., Pernier, J., Bertrand, O., & Echallier, J. F. (1989). Spherical splines for scalp potential and current density mapping. *Electroencephalography and Clinical Neurophysiology*, 72, 184–187. **DOI:** [https://doi.org/10.1016/0013-4694\(89\)90180-6](https://doi.org/10.1016/0013-4694(89)90180-6)
- Pfurtscheller, G., Graimann, B., Huggins, J. E., Levine, S. P., & Schuh, L. A. (2003). Spatiotemporal patterns of  $\beta$  desynchronization and gamma synchronization in corticographic data during self-paced movement. *Clinical Neurophysiology*, 114, 1226–1236. **DOI:** [https://doi.org/10.1016/S1388-2457\(03\)00067-1](https://doi.org/10.1016/S1388-2457(03)00067-1)
- Pfurtscheller, G., Neuper, C., Brunner, C., & Da Silva, F. L. (2005). Beta rebound after different types of motor imagery in man. *Neuroscience Letters*, 378, 156–159. **DOI:** <https://doi.org/10.1016/j.neulet.2004.12.034>, **PMID:** 15781150
- Pfurtscheller, G., Neuper, C., Flotzinger, D., & Peregnyer, M. (1997). EEG-based discrimination between imagination of right and left hand movement. *Electroencephalography and Clinical Neurophysiology*, 103, 642–651. **DOI:** [https://doi.org/10.1016/S0013-4694\(97\)00080-1](https://doi.org/10.1016/S0013-4694(97)00080-1)
- Pogosyan, A., Gaynor, L. D., Eusebio, A., & Brown, P. (2009). Boosting cortical activity at  $\beta$ -band frequencies slows movement in humans. *Current Biology*, 19, 1637–1641. **DOI:** <https://doi.org/10.1016/j.cub.2009.07.074>, **PMID:** 19800236, **PMCID:** PMC2791174
- Raud, L., Huster, R., Ivry, R. B., Labruna, L., Messel, M. S., & Greenhouse, I. (2020). A single mechanism for global and selective response inhibition under the influence of motor preparation. *Journal of Neuroscience*, 40, 7921–7935. **DOI:** <https://doi.org/10.1523/JNEUROSCI.0607-20.2020>, **PMID:** 32928884, **PMCID:** PMC7548697
- Ridderinkhof, R. K. (2002). Micro- and macro-adjustments of task set: Activation and suppression in conflict tasks. *Psychological Research*, 66, 312–323. **DOI:** <https://doi.org/10.1007/s00426-002-0104-7>, **PMID:** 12466928
- Ridderinkhof, K. R., de Vlugt, Y., Bramlage, A., Spaan, M., Elton, M., Snel, J., et al. (2002). Alcohol consumption impairs detection of performance errors in mediofrontal cortex. *Science*, 298, 2209–2211. **DOI:** <https://doi.org/10.1126/science.1076929>, **PMID:** 12424384
- Ridderinkhof, K., Forstmann, B. U., Wylie, S. A., Burle, B., & van den Wildenberg, W. P. M. (2011). Neurocognitive mechanisms of action control: Resisting the call of the Sirens. *Wiley Interdisciplinary Reviews: Cognitive Science*, 2, 174–192. **DOI:** <https://doi.org/10.1002/wcs.99>, **PMID:** 26302009
- Robbins, T. W. (2007). Shifting and stopping: Fronto-striatal substrates, neurochemical modulation and clinical implications. *Philosophical Transactions of the Royal Society of London, Series B, Biological Sciences*, 362, 917–932. **DOI:** <https://doi.org/10.1098/rstb.2007.2097>, **PMID:** 17412678, **PMCID:** PMC2430006
- Schmidt, R., & Berke, J. D. (2017). A pause-then-cancel model of stopping: Evidence from basal ganglia neurophysiology. *Philosophical Transactions of the Royal Society of London, Series B, Biological Sciences* 372, 20160202. **DOI:** <https://doi.org/10.1098/rstb.2016.0202>

- doi.org/10.1098/rstb.2016.0202, **PMID:** 28242736, **PMCID:** PMC5332861
- Schoffelen, J.-M., Oostenveld, R., & Fries, P. (2008). Imaging the human motor system's  $\beta$ -band synchronization during isometric contraction. *Neuroimage*, *41*, 437–447. **DOI:** <https://doi.org/10.1016/j.neuroimage.2008.01.045>, **PMID:** 18396062
- Schulz, H., Übelacker, T., Keil, J., Müller, N., & Weisz, N. (2013). Now I am ready—Now I am not: The influence of pre-TMS oscillations and corticomuscular coherence on motor-evoked potentials. *Cerebral Cortex*, *24*, 1708–1719. **DOI:** <https://doi.org/10.1093/cercor/bht024>, **PMID:** 23395847
- Sherman, M. A., Lee, S., Law, R., Haegens, S., Thorn, C. A., Hämäläinen, M. S., et al. (2016). Neural mechanisms of transient neocortical  $\beta$  rhythms: Converging evidence from humans, computational modeling, monkeys, and mice. *Proceedings of the National Academy of Sciences, U.S.A.*, *113*, E4885–E4894. **DOI:** <https://doi.org/10.1073/pnas.1604135113>, **PMID:** 27469163, **PMCID:** PMC4995995
- Shin, H., Law, R., Tsutsui, S., Moore, C. I., & Jones, S. R. (2017). The rate of transient  $\beta$  frequency events predicts behavior across tasks and species. *eLife*, *6*, e29086. **DOI:** <https://doi.org/10.7554/eLife.29086>, **PMID:** 29106374, **PMCID:** PMC5683757
- Swann, N. C., Cai, W., Conner, C. R., Pieters, T. A., Claffey, M. P., George, J. S., et al. (2012). Roles for the pre-supplementary motor area and the right inferior frontal gyrus in stopping action: Electrophysiological responses and functional and structural connectivity. *Neuroimage*, *59*, 2860–2870. **DOI:** <https://doi.org/10.1016/j.neuroimage.2011.09.049>, **PMID:** 21979383, **PMCID:** PMC3322194
- Tan, H., Wade, C., & Brown, P. (2016). Post-movement  $\beta$  Activity in sensorimotor cortex indexes confidence in the estimations from internal models. *Journal of Neuroscience*, *36*, 1516–1528. **DOI:** <https://doi.org/10.1523/JNEUROSCI.3204-15.2016>, **PMID:** 26843635, **PMCID:** PMC4737767
- Tenke, C. E., & Kayser, J. (2005). Reference-free quantification of EEG spectra: Combining current source density (CSD) and frequency principal components analysis (fPCA). *Clinical Neurophysiology*, *116*, 2826–2846. **DOI:** <https://doi.org/10.1016/j.clinph.2005.08.007>, **PMID:** 16257577
- Tinkhauser, G., Pogosyan, A., Little, S., Beudel, M., Herz, D. M., Tan, H., et al. (2017). The modulatory effect of adaptive deep brain stimulation on  $\beta$  bursts in Parkinson's disease. *Brain*, *140*, 1053–1067. **DOI:** <https://doi.org/10.1093/brain/awx010>, **PMID:** 28334851, **PMCID:** PMC5382944
- Tzagarakis, C., West, S., & Pellizzer, G. (2015). Brain oscillatory activity during motor preparation: Effect of directional uncertainty on  $\beta$ , but not alpha, frequency band. *Frontiers in Neuroscience*, *9*, 246. **DOI:** <https://doi.org/10.3389/fnins.2015.00246>, **PMID:** 26257597, **PMCID:** PMC4508519
- Ullsperger, M., & Danielmeier, C. (2016). Reducing speed and sight: How adaptive is post-error slowing? *Neuron*, *89*, 430–432. **DOI:** <https://doi.org/10.1016/j.neuron.2016.01.035>, **PMID:** 26844827
- Verbruggen, F., Aron, A. R., Band, G. P., Beste, C., Bissett, P. G., Brockett, A. T., et al. (2019). A consensus guide to capturing the ability to inhibit actions and impulsive behaviors in the stop-signal task. *eLife*, *8*, e46323. **DOI:** <https://doi.org/10.7554/eLife.46323>, **PMID:** 31033438, **PMCID:** PMC6533084
- Verbruggen, F., & Logan, G. D. (2009). Proactive adjustments of response strategies in the stop-signal paradigm. *Journal of Experimental Psychology: Human Perception and Performance*, *35*, 835–854. **DOI:** <https://doi.org/10.1037/a0012726>, **PMID:** 19485695, **PMCID:** PMC2690716
- Vink, M., Kaldewaij, R., Zandbelt, B. B., Pas, P., & du Plessis, S. (2015). The role of stop-signal probability and expectation in proactive inhibition. *European Journal of Neuroscience*, *41*, 1086–1094. **DOI:** <https://doi.org/10.1111/ejn.12879>, **PMID:** 25832122
- Wessel, J. R. (2018). Surprise: A more realistic framework for studying action stopping? *Trends in Cognitive Sciences*, *22*, 741–744. **DOI:** <https://doi.org/10.1016/j.tics.2018.06.005>, **PMID:** 30122169, **PMCID:** PMC7714639
- Wessel, J. R. (2020).  $\beta$ -bursts reveal the trial-to-trial dynamics of movement initiation and cancellation. *Journal of Neuroscience*, *40*, 411–423. **DOI:** <https://doi.org/10.1523/JNEUROSCI.1887-19.2019>, **PMID:** 31748375, **PMCID:** PMC6948942
- Wessel, J. R., & Aron, A. R. (2017). On the globality of motor suppression: Unexpected events and their influence on behavior and cognition. *Neuron*, *93*, 259–280. **DOI:** <https://doi.org/10.1016/j.neuron.2016.12.013>, **PMID:** 28103476, **PMCID:** PMC5260803
- Wessel, J. R., Conner, C. R., Aron, A. R., & Tandon, N. (2013). Chronometric electrical stimulation of right inferior frontal cortex increases motor braking. *Journal of Neuroscience*, *33*, 19611–19619. **DOI:** <https://doi.org/10.1523/JNEUROSCI.3468-13.2013>, **PMID:** 24336725, **PMCID:** PMC3858630
- Wessel, J. R., Waller, D. A., & Greenlee, J. D. W. (2019). Non-selective inhibition of inappropriate motor-tendencies during response-conflict by a fronto-subthalamic mechanism. *eLife*, *8*, e42959. **DOI:** <https://doi.org/10.7554/eLife.42959>, **PMID:** 31063130, **PMCID:** PMC6533064
- van den Wildenberg, W. P. M., van Boxtel, G. J. M., van der Molen, M. W., Bosch, D. A., Speelman, J. D., & Brunia, C. H. M. (2006). Stimulation of the subthalamic region facilitates the selection and inhibition of motor responses in Parkinson's disease. *Journal of Cognitive Neuroscience*, *18*, 626–636. **DOI:** <https://doi.org/10.1162/jocn.2006.18.4.626>, **PMID:** 16768365
- Zandbelt, B. B., & Vink, M. (2010). On the role of the striatum in response inhibition. *PLoS One*, *5*, e13848. **DOI:** <https://doi.org/10.1371/journal.pone.0013848>, **PMID:** 21079814, **PMCID:** PMC2973972
- Zhang, Y., Chen, Y., Bressler, S. L., & Ding, M. (2008). Response preparation and inhibition: The role of the cortical sensorimotor  $\beta$  rhythm. *Neuroscience*, *156*, 238–246. **DOI:** <https://doi.org/10.1016/j.neuroscience.2008.06.061>, **PMID:** 18674598, **PMCID:** PMC2684699